Stochastic Langevin Model for Flow and Transport in Porous Media

Alexandre M. Tartakovsky*
Pacific Northwest National Laboratory, Richland, Washington 99352, USA

Daniel M. Tartakovsky†
University of California San Diego, La Jolla, California 92093, USA

Paul Meakin‡
Idaho National Laboratory, Idaho Falls, Idaho 83415, USA

(Received 26 November 2007; revised manuscript received 27 April 2008; published 22 July 2008)

We present a new model for fluid flow and solute transport in porous media, which employs smoothed particle hydrodynamics to solve a Langevin equation for flow and dispersion in porous media. This allows for effective separation of the advective and diffusive mixing mechanisms, which is absent in the classical dispersion theory that lumps both types of mixing into dispersion coefficient. The classical dispersion theory overestimates both mixing-induced effective reaction rates and the effective fractal dimension of the mixing fronts associated with miscible fluid Rayleigh-Taylor instabilities. We demonstrate that the stochastic (Langevin equation) model overcomes these deficiencies.

DOI: 10.1103/PhysRevLett.101.044502 PACS numbers: 47.56.+r, 05.10.Gg

Flow and transport in porous media can be described on two fundamental scales. On the pore scale, these phenomena are governed by the Navier-Stokes and advection-diffusion equations. Detailed knowledge of the pore geometry of most natural and manufactured porous media is elusive, and solving these equations over a large volume of a porous medium is often computationally prohibitive. These and other practical considerations have led to the development of continuum (or Darcy-scale) models, which are obtained by averaging the Navier-Stokes and/or advection-diffusion equations over a sufficiently large volume of the porous medium.

After a series of simplifying assumptions, the volumetric or statistical averaging of the pore-scale continuity and Navier-Stokes equations yields [1] the Darcy-scale continuity equation

$$\frac{d\rho}{dt} = -\rho\nabla\cdot\mathbf{u} \tag{1}$$

and the Darcy-scale momentum conservation equation

$$\frac{d\mathbf{u}}{dt} = -\frac{\nabla p}{\rho} + \mathbf{g} - \gamma\mathbf{u}. \tag{2}$$

Here $d/dt \equiv \partial/\partial t + \mathbf{u}\cdot\nabla$ denotes the material derivative, $\mathbf{u}$ is the mean microscopic velocity of a fluid with density ρ and viscosity μ, $\mathbf{g}$ is the gravitational acceleration, and p is the pressure. The friction coefficient $\gamma = \phi\mu/(\rho k)$, porosity ϕ, permeability k and hydraulic conductivity $\phi g/\gamma$ are some of the macroscopic parameters characterizing porous media on the Darcy scale. While it is common to simplify (2) further by setting $d\mathbf{u}/dt$ to 0, which gives rise to Darcy's law, we retain this term for completeness.

A similar averaging procedure applied to the pore-scale advection-diffusion equation gives rise to the Darcy-scale advection-dispersion equation (ADE) [1]

$$\rho\frac{dC}{dt} = \nabla\cdot(D\rho\nabla C). \tag{3}$$

Here C is the solute concentration defined as a mass of solute per unit mass of a solution, $D = D_m/\tau + \alpha|\mathbf{u}|$ is the dispersion coefficient written as a scalar rather than a tensor to simplify the presentation, D_m is the molecular diffusion coefficient, and τ and α are the tortuosity and the dispersivity of the porous medium.

While adequate in many settings, the classical Darcy-scale equations (1)–(3) have a number of known conceptual and operational drawbacks. For example, (3) implies that hydrodynamic dispersion is functionally analogous to Fickian diffusion with a macro-scale effective diffusion coefficient D that lumps together advective mixing (spreading due to variations in the fluid velocity) and diffusive mixing [1]. This contradicts a number of observations, which indicate that dispersive mixing is fundamentally different from its purely diffusive counterpart. Specifically, the fractal dimensions of the diffusion and dispersion fronts (isoconcentration contours) are different [2], and ADE-based models of reactive transport can significantly over-predict the extent of reaction in mixing-induced chemical transformations [3–5].

In heterogeneous porous media, many of the shortcomings of the traditional ADE can be overcome by treating the hydraulic conductivity or, equivalently, the mean microscopic velocity $\mathbf{u}$ in (3) as random fields and applying either stochastic averaging (e.g., [6]) or renormalization-group analyses (e.g., [7]). According to these and other similar approaches, the randomness is absent if the porous medium is homogeneous and the drawbacks of the ADE (3) reemerge.

In this Letter, we introduce a new stochastic Lagrangian model for flow and transport in porous media that allows one to separate advective mixing from its diffusive counterpart. The model posits that fluid flow in homogeneous porous media is governed by a combination of the continuity equation (1) and a stochastic Langevin flow equation which is obtained by adding white noise fluctuations $\boldsymbol{\xi}$ to the macroscopic flow equation (2). In this mesoscale formulation, the noise represents the subgrid variability of the flow velocity and the combined effects of the simplifying assumptions leading to (2), and accounts for deviations from the smooth flow paths predicted by the Darcy-scale continuum flow equations (1) and (2). This is conceptually analogous to the role played by the noise in Brownian motion models of diffusion and in fluctuating hydrodynamics [8].

The resulting stochastic flow and transport equations can be solved by a variety of methods. Here we solve them with smoothed particles hydrodynamics (SPH), a Lagrangian numerical algorithm that has been successfully applied to both deterministic [9,10] and stochastic [11] transport problems. In SPH the fluid is represented with M particles, and the stochastic Langevin flow equation is

$$\frac{d\mathbf{U}_i}{dt} = -\frac{\nabla P_i}{\rho_i} + \mathbf{g} - \gamma_i \mathbf{U}_i + \sqrt{|\langle \mathbf{U}_i \rangle|}\boldsymbol{\xi}, \qquad \frac{d\mathbf{X}_i}{dt} = \mathbf{U}_i, \tag{4}$$

where the subscript i ($i = 1, \ldots, M$) indicates the random position $\mathbf{X}$, velocity $\mathbf{U}$, and pressure P of the ith particle. Reynolds' decomposition is used to represent a random quantity $\mathcal{A}$ ($= \mathbf{X}, \mathbf{U}, P$) as the sum $\mathcal{A} = \langle \mathcal{A} \rangle + \tilde{\mathcal{A}}$ of its ensemble mean $\langle \mathcal{A} \rangle$ and random fluctuations about the mean $\tilde{\mathcal{A}}$. The components of the white noise $\boldsymbol{\xi} = (\xi_1, \ldots, \xi_d)^T$ satisfy $\langle \xi_l(t) \rangle = 0$ ($l = 1, \ldots, d$, where d is the system's dimensionality) and

$$\langle \xi_l(t) \xi_m(t') \rangle = \begin{cases} \Gamma_{ll}^2 \delta(t - t'), & l = m \\ 0, & \text{otherwise.} \end{cases} \tag{5}$$

For simplicity, and without any loss of generality, we set the constants $\Gamma_{ll} = \Gamma$ for all l. This is consistent with taking the dispersivity α to be a scalar. The variance of the ith particle's position can be related to the dispersivity via Einstein's relationship

$$\lim_{t \to \infty} \frac{d\langle \tilde{X}_{l,i}(t) \tilde{X}_{l,i}(t) \rangle}{dt} = 2\alpha |\langle \mathbf{U}_i \rangle^{\infty}|, \tag{6}$$

where $\langle \mathbf{U}_i \rangle^{\infty}$ is the steady average velocity of the ith particle. In the stochastic simulations presented here, the values of the parameter Γ was set to 0.046. Figure 1 shows the variances of the x and y components of the particle position vector, $\langle \tilde{X}_l^2(t) \rangle$, versus time for the stochastic simulation with $\langle \mathbf{U_i} \rangle^{\infty} = 1$ from which a value of 0.02 was obtained for α using Eq. (6). The simulation was performed in a two-dimensional rectangular periodic domain filled with $M = 8192$ fluid particles. The flow was driven by gravitational body forces acting on the SPH fluid particles. Because of the periodic boundary conditions, all the fluid particles were statistically equivalent, and the variance of the deviate of the position of any particle i was the same and could be found from $\langle \tilde{X}_l^2(t) \rangle = 1/M \sum_1^M (X_{l,i} - \langle X_{l,i} \rangle)^2$. The proposed Langevin model of flow and transport in porous media allows one to elucidate the relative effects of dispersive and diffusive mixing. This is because molecular diffusion can be described explicitly by the classical advection-diffusion equation,

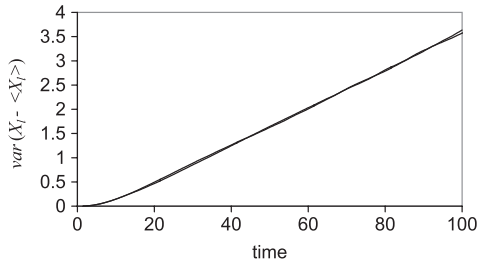

FIG. 1. Variances $\langle \tilde{X}_1^2(t) \rangle$ (solid line) and $\langle \tilde{X}_1^2(t) \rangle$ (broken line) of the x_1 and x_2 components of the particles position vector $\mathbf{X}(t)$, respectively.

$$\rho \frac{dC}{dt} = \nabla \cdot (\rho D_m \nabla C), \tag{7}$$

where $dC/dt = \partial C/\partial t + \mathbf{U} \cdot \nabla \mathbf{C}$, and $\mathbf{U}$ is the stochastic velocity found from Eq. (4). To demonstrate the key ideas behind our model and to contrast it with the standard deterministic alternative, we used the two models to simulate three transport phenomena: transport of a conservative tracer, multicomponent reactive transport, and density-driven unstable miscible flow. For consistency, the solution of deterministic equations (1)–(3) was also obtained with SPH.

Transport of a passive scalar.—The first example deals with transport of a conservative tracer in a two-dimensional rectangular domain. Figure 2 provides a snapshot of a plume migrating through a homogeneous porous medium, for the Péclet number $\mathrm{Pe} = |\langle \mathbf{U} \rangle| L/D_m = 1.7 \times 10^5$, L being the size of the domain in the flow direction. The upper figure was obtained using the standard ADE model and the lower was obtained using the stochastic model. The ADE model yields a well mixed plume, while the stochastic advection-diffusion equation predicted highly nonuniform transport of solute. Similar nonuniform mixing has been observed experimentally (e.g., [2]). The effect of nonuniform mixing is especially important in coupled processes, such as multicomponent reactions and Rayleigh-Taylor instability simulated below.

Reactive transport.—In the second example, we consider transport of two solutes $\mathcal{A}$ and $\mathcal{B}$ undergoing a homogenous second-order reaction $\mathcal{A} + \mathcal{B} \rightarrow \mathcal{C}$ in the aqueous phase. The concentrations A, B, and C of the compounds $\mathcal{A}$, $\mathcal{B}$, and $\mathcal{C}$ evolve according to the

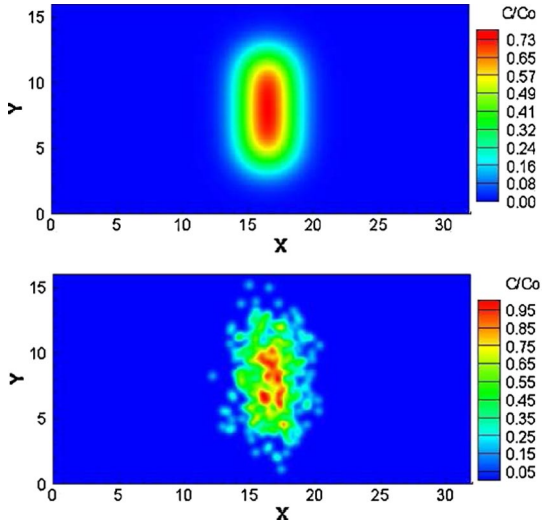

FIG. 2 (color online). Deterministic and stochastic simulations of solute diffusion and dispersion.

Lagrangian transport equations

$$\frac{dI}{dt} = \frac{1}{\rho}\nabla \cdot (\rho K \nabla I) - kAB,$$
$$\frac{dC}{dt} = \frac{1}{\rho}\nabla \cdot (\rho K \nabla C) + kAB, \tag{8}$$

where $I = A, B$. Constant concentrations A_0 and B_0 are prescribed along the upper and lower halves of the left boundary of the rectangular flow domain, respectively. The concentration gradients of $\mathcal{A}$, $\mathcal{B}$, and $\mathcal{C}$ at the right boundary are set to zero. The flow is driven by a (gravitational) body force acting from left to right. Periodic boundary conditions are imposed along the vertical boundaries, and the horizontal boundaries are treated as impermeable. In the stochastic model, the advective velocity in equation (8) is given by (1) and (4) and $K \equiv D_m$. In the deterministic model, the advective velocity in (8) is found from (1) and (2) and $K \equiv D$. Figure 3 shows the concentration of the reaction product C/C_0 ($C_0 \equiv A_0 = B_0$), computed with the deterministic and stochastic simulations in which the fluid was discretized with $M = 8192$ particles. The deterministic model predicts that the mixing zone widens uniformly in the direction of flow, and that the concentration C varies smoothly in the mixing zone. The stochastic model yields a nonuniform distribution of C in the mixing zone.

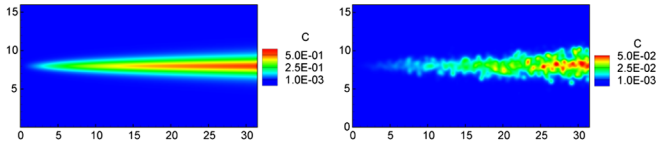

FIG. 3 (color online). Deterministic (above) and stochastic (below) predictions of the concentration C of the reaction product $\mathcal{C}$.

The latter behavior is more physical, since the large Péclet number (Pe $= 1.7 \times 10^5$), i.e., the small diffusion coefficient, used in these simulations precludes the complete mixing of solutes $\mathcal{A}$ and $\mathcal{B}$. Figure 4 exhibits the evolution of the total dimensionless mass of $\mathcal{C}$ predicted by the deterministic and stochastic models. The deterministic model overestimates the mass and the maximum concentration of reaction product C by an order of magnitude. The difference in the stochastic solutions, obtained with 8192 and 18432 particles, was less than 2%.

Rayleigh-Taylor instability.—In the final example, we consider a Rayleigh-Taylor (RT) instability induced by the miscible displacement of a less dense fluid by a more dense fluid (e.g., when overlying brine displaces water). We assume that both the density ρ and viscosity μ of a fluid vary linearly with the solute concentration, $\rho = \rho_0 + k^\rho C$ and $\mu = \mu_0 + k^\mu C$, where ρ_0 and μ_0 are the fluid's density and viscosity in the absence of the solute. The deterministic model consists of (1)–(3) with $\alpha = 0.02$, and the stochastic model is based on (1) and (4) with $\Gamma = 0.046$, and (7). The initial solute concentration was C_0 in the upper half of the computational domain and zero in the lower half of the domain. The flow is driven by the gravitational force acting downward. The simulations were conducted in a two-dimensional square domain with impermeable boundaries. A snapshot of these simulations is presented in Fig. 5. For both models, the isoconcentration contours of the fronts separating the denser and lighter fluids exhibit fractal geometry (Fig. 6). The deterministic model predicts a smoother front whose effective fractal dimension is $D_f \approx 1.23$, while its stochastic counterpart results in a rougher front with an effective fractal dimension of $D_f \approx 1.32$. The fractal dimension was determined via a box-counting analysis (BCA), with the front defined as the region where $C/C_0 \in [0.4, 0.6]$. The BCA determines the fractal dimension from the relationship $N(s) \sim (1/s)^{D_f}$, where $N(s)$ is the number of boxes of size s, needed to cover the front [Fig. 6(a)]. Also, the stochastic model produces a front with a higher density gradient and a higher propagation rate than the front predicted from the deterministic model [Fig. 6(b)].

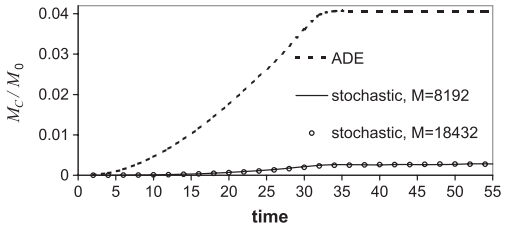

FIG. 4. Evolution of the total mass of $\mathcal{C}$ (normalized with $M_0 = C_0 M_T$ where M_T is the total mass of fluid particles in the computational domain), predicted by the deterministic (dashed line) and stochastic models with 8192 (solid line) and 18432 (open circles) SPH particles.

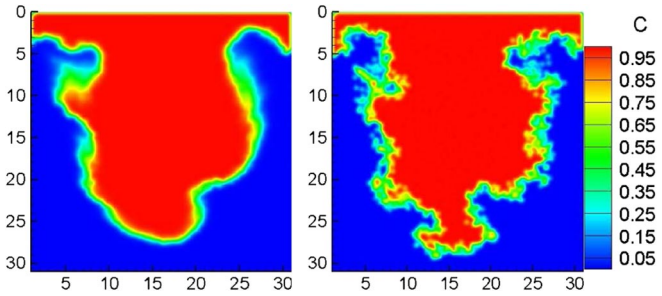

FIG. 5 (color online). Deterministic (left) and stochastic (right) predictions of the Rayleigh-Taylor density-driven instability.

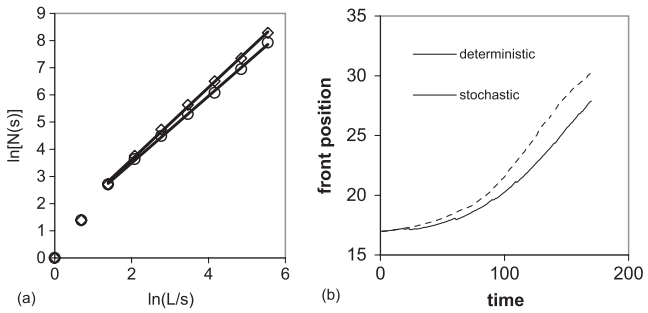

FIG. 6. (a) The number of boxes $N(s)$ needed to cover the concentration isosurface $C/C_0 = 0.5$ corresponding to the deterministic (circles) and stochastic models (diamonds) shown in Fig. 5 as a function of the box size s/L, where L is the size of the computational domain. The fractal dimension is estimated as the slope of the linear part of the curves. (b) Position of the front (tip of the isosurface $C/C_0 = 0.5$) as a function of time predicted by the two models.

Summary.—We presented a new Lagrangian stochastic model for flow and transport in porous media. The pore-scale variability of the fluid velocity enters the macroscopic (Darcy scale) equations as random noise. The composition of the liquid particles does not change as a result of particle advection, but it does change as a result of diffusion. The stochastic model obviates the need for a constitutive relation for the dispersion coefficient by separating the effects of diffusive and advective mixing on solute transport, while the classical ADE-based models assume that fluid particles move with the mean flow velocity (no dispersion of fluid particles), and treat solute dispersion as a macrodiffusion process. The two approaches were used to model transport of a conservative tracer, multicomponent reactive transport, and the Rayleigh-Taylor instability. For large Péclet numbers, which are ubiquitous in field-scale transport, the ADE-based models are known to overestimate solute mixing, produce artificially smooth concentration profiles, significantly overestimate the concentrations of the product of chemical reactions, and underestimate the effective fractal dimension and propagation rate of the fronts with the Rayleigh-Taylor instability. The presented model alleviates these shortcomings. It is worthwhile emphasizing the fundamental differences between the proposed stochastic flow and transport model and the existing stochastic diffusion or dispersion models, which use Langevin equations to represent random walk processes on both pore- and Darcy scales (e.g., [12].) In our model, random velocities of adjacent fluid particles are correlated through the continuity equation, while the velocities of random walkers (tracer particles) are not. Finally, since SPH particles serve as discretization points for governing partial differential equations, the proposed approach provides a natural framework for dealing with such transport mechanisms as molecular diffusion and chemical kinetics, as well as with coupled flow and transport processes (e.g., variable density flow).

This work was supported by the Advanced Scientific Computing Research Program and the Environmental Management Science Program of the U.S. Department of Energy Office of Science. The Pacific Northwest National Laboratory is operated for the U. S. Department of Energy by Battelle under Contract No. DE-AC05-76RL01830.

*alexandre.tartakovsky@pnl.gov
†dmt@ucsd.edu
‡paul.meakin@inl.gov

[1] J. Bear and Y. Bachmat, *Introduction to Modeling of Transport Phenomena in Porous Media* (Kluwer Academic, New York, 1990).
[2] K. Maloy, J. Feder, F. Boger, and T. Jossang, Phys. Rev. Lett. **61**, 2925 (1988).
[3] C. Knutson, A. Valocchi, and C. Werth, Adv. Water Resour. **30**, 1421 (2007).
[4] O. Cirpka, E. Frind, and R. Helmig, J. Contam. Hydrol. **40**, 159 (1999).
[5] M. Widdowson, F. Molz, and L. Benefield, Water Resour. Res. **24**, 1553 (1988).
[6] D. Koch and J. Brady, J. Fluid Mech. **154**, 399 (1985).
[7] J. Aranovitz and D. Nelson, Phys. Rev. A **30**, 1948 (1984).
[8] J. O. de Zarate and J. Sengers, *Hydrodynamic Fluctuations in Fluids and Fluid Mixtures* (Elsevier, New York, 2006).
[9] J. Monaghan, Rep. Prog. Phys. **68**, 1703 (2005).
[10] A. Tartakovsky and P. Meakin, J. Comput. Phys. **207**, 610 (2005).
[11] W. Welton and S. Pope, J. Comput. Phys. **134**, 150 (1997).
[12] R. Mayer, D. Kroll, R. Bernard, S. Howington, J. Peters, and H. Davis, Phys. Fluids **12**, 2065 (2000).